Ceramics International 49 (2023) 37118–37126

Contents lists available at ScienceDirect

Ceramics International

journal homepage: www.elsevier.com/locate/ceramint

Assessment of different optimized anti-reflection coatings for ZnO/Si heterojunction solar cells

Sameen Maqsood [a,b], Zohaib Ali [a], Khuram Ali [a,***], Mubashra Ishaq [c], Muhammad Sajid [a], Ahmad Farhan [d], Abbas Rahdar [e,**], Sadanand Pandey [f,g,*]

[a] Nano-optoelectronics Research Laboratory, Department of Physics, University of Agriculture Faisalabad, Faisalabad, 38040, Pakistan
[b] Department of Physics, Government College Women University, Faisalabad, Pakistan
[c] Riphah International University, Faisalabad, Pakistan
[d] Department of Chemistry, University of Agriculture, Faisalabad, 38040, Pakistan
[e] Department of Physics, University of Zabol, Zabol, 98613-35856, Iran
[f] School of Bioengineering & Food Technology, Shoolini University, Solan, Himachal Pradesh, 173229, India
[g] Department of Chemistry, College of Natural Science, Yeungnam University, 280 Daehak-Ro, Gyeongsan, 38541, South Korea

ARTICLE INFO

Handling Editor: Dr P. Vincenzini

Keywords:
Antireflection materials
PC1D simulation
ZnO/Si solar cells
Power conversion efficiency
Optoelectrical properties

ABSTRACT

The heterojunction (HJ) solar cell is one of the superlative alternatives to upgrade traditional single homojunction silicon-based solar cells. The present paper reports on the simulation investigation for examining the high-performance Zinc oxide (ZnO)/Si solar cells with different anti-reflection coatings (ARC), optimizing the absorber, window thickness, and ARC layers. In this study, the parameters were selected, like ZnO as a window layer, Si as an absorber layer, and the thickness of different ARC layers to perform PC1D (personal computer one dimensional) simulation. Aluminum trioxide (Al_2O_3), Magnesium oxide (MgO), Magnesium fluoride (MgF_2), and Titanium nitrate (TIN) were used as a single layer. Without any ARC layer, 18.8% power conversion efficiency (PCE) and 21.3% PCE were recorded for ZnO/Si solar cells at zero reflectance. The MgF_2 as a single ARC layer of 110 nm thickness has achieved a PCE of 20.8% compared to other anti-reflection coating materials at an absorber layer of 160 μm and window layer of 0.5 μm. The optimized value of carrier lifetime was found to be 100μs for ARC layers. The values of PCE, Voc and Isc gradually increased with increasing carrier lifetime. The maximum values of Voc = 0.6580, Isc = 0.0386 A and PCE with 20.8% were achieved by MgF_2 ARC layer at optimized parameters.

1. Introduction

Humankind has been dealing with increasingly complicated environmental concerns and a massive energy crisis since the 21st century. Solar cells play a significant role in the global energy industry because of their long-term sustainability and environmental friendliness [1]. Semiconductors, particularly transparent conductive oxides (TCO), have a large bandgap, good transmittance in the visible range and DC resistivity up to 10^{-5}-10^{-4} Ω cm (n-type). They are generally utilized as front electrodes in thin-film photovoltaic cells [2]. The most prevalent TCO thin films include binary and ternary oxides and their various doping systems like ZnO, CdO, SnO_2,In_2O_3, Cu_2O, Ga_2O_3, and $SrTiO_3$. The d-electron orbitals of elements (Cd, Sn, Zn, In) are filled when they react with oxygen, a fundamental property of a binary oxide system [3]. Highly transparent tungsten oxides with low conductivity can be utilized at the visible side to achieve higher current density.

Establishing hole contact in an heterojunction is usually more delicate than electron contact [4]. Zinc oxide is a promising candidate as transparent conductive oxides (TCO) layer in the PV industry due to low toxicity, low cost, low deposition temperature, abundance and lower production cost [5,6]. Moreover, n-type Zinc oxide is found to be useful in optical devices as well as PV cells. Numerous researchers use n-ZnO thin films as anti-reflection coating and emitter layer to fabricate low-cost, high-efficiency solar cells [7]. Considering the optical

* Corresponding author. School of Bioengineering & Food Technology, Shoolini University, Solan, Himachal Pradesh, 173229, India.
** Corresponding author.
*** Corresponding author.
E-mail addresses: khuram_uaf@yahoo.com (K. Ali), a.rahdar@uoz.ac.ir (A. Rahdar), Sadanand.au@gmail.com (S. Pandey).

https://doi.org/10.1016/j.ceramint.2023.08.313
Received 7 July 2023; Received in revised form 11 August 2023; Accepted 28 August 2023
Available online 29 August 2023

properties of zinc oxide thin film as an n-layer, the front ZnO thin film is designed to operate as an electrically active layer and as an ARC layer to producea p-n junction. The benefits of heterojunction solar cells are the dopant concentration, flexibility to choose a material, low-temperature approach, intrinsic surface passivation and layer thickness [8].

As a result, solar cells based on zinc oxide silicon heterojunction may be more competitive in the future PV industry. Various researchers have also demonstrated single Si heterojunction-based solar cells produced from metal oxides. Gerling et al. [9] designed a solar cell based on a single heterojunction by applying thermally evaporated four TCO(WO_3, V_2O_5, MoO_3) with high work functions as front contact in planar n-Si solar cells. Among these TCOs, V_2O_5 provides the highest PCE of 12.7% with V_{oc} of 593 mV compared to WO_3 and MoO_3 as p-layer. Furthermore, solar cells based on NiO_2/Si heterojunction fabricated with NiO_2 asp-layer and as active absorption layer n-type silicon were used efficiency of 12.73% and increment in V_{oc} from 423 to 906.16 mV reported with the increment of NiO_2 layer was achieved [10]. Solar cells based on c-Si heterojunction have recently received a lot of attention due to low-temperature impact on conversion efficiency and slow fabrication cost [11,12], and low fabrication temperature [13]. Heterojunction cells employ c-Si substrate as an emitter with a large band gap of hydrogenated a-Si, and carriers can move in unidirectional because of a larger band offset [14]. Chen et al. [15] used the metal-organic chemical vapor deposition method to deposit boron-doped ZnO thin films and AFORS-HET tools to do computational research of ZnO/Si solar cells. The ZnO layer was used as emitter on the Si wafer, and I = 0.302 A, PCE of 17.16%, V_{oc} = 0.675 V and FF of 83.96% were recorded. Ziani and Belkaid [16] used a SCAPS-1D simulator and reported similar ZnO/Si based solar cell performances. Pietruszka et al. [17] achieved 14% PCE with ZnO/Si solar cells by using the atomic layer deposition method. Shah et al. [18]. used PCID to explore the optical properties of the silver-doped ZnO/ZnO double ARC layer in terms of surface charge carrier concentrations and minority charge carriers. The Silicon based solar cell with Ag–ZnO/ZnO double ARC possess highest conversion efficiency of 15.32% with fill factor (FF) of 81.35% at doping carrier concentration of 1×10^{17} cm^{-3} and minority carrier lifetime of 10 μs when compared to single anti-reflection layer. Spray pyrolysis were used to prepare nickel (Ni) doped ZnO thin films, resulting in an optical bandgap reduction from 3.47 eV to 2.87 eV for undoped ZnO film with 15% Ni doping [19]. Vallisree et al. [20] reported that introduction of Mg in ZnO can enhance efficiency up to 14.46% by using Silvaco ATLAS simulator. Tyagi et al. [21] introduces graphene with ZnO to make it hybrid sole cell and uses SCAPS 1D to investigate the performance. PCE of 8.46%, 52.14% FF, 12.46 mA/cm^2, Jsc and 0.79 V Voc achieved by simulated analysis. Boudour et [22] uses AMPS-1D simulator to investigate the ZnO/Si/Cu_2O based solar cell. 16.23% conversion efficiency has been attained through this heterojunction. Askari et al. [23] used TCAD software to study the interface characteristics of ZnO/Si solar cells and achieved approximately 14% efficiency. Chen et al. [15] used AFORS-HET software and provide experimental verification of ZnO/Si solar cell. MOCVD used to deposit the ZnO layer on p-Si wafer. The reported PCE of 17.6 5 via simulation and 2.82% by fabrication of solar cell. Gulomov et al. [24]investigated the optical and electrical properties of TiO_2/Si and ZnO/Si. Reported FF of TiO_2/Si and ZnO/Si based solar cells was 0.76 and 0.73. So ZnO can be used as emitter layer and TiO_2 as transparent contact for Si based solar cells. Mandal et al. [25] used SCAPS-1D simulator to study the defects between Si and ZnO. 15.42% PCE with 541 mV Voc for low defect density (10^{10} cm^{-2}). Decrement in efficiency notices with the increment in defect density. Das et al. [26] used silicon doped ZnO as TCO layer for p-Si based cell. Reported values of transmittance and resistivity are 5.0×10^{-3} Ω cm 89%.RF magnetron sputtering technique was used to achieve these values.

Optical and electrical losses must be decreased to attain maximum conversion efficiency [27]. In photovoltaic devices one of the main challenges is to reduce the optical losses, which is responsible for approximately 4% of the efficiency reduction in c-Si solar cells [28]. Antireflective coatings (ARCs) are a crucial component for achieving optimum conversion efficiency and excellent performance. An ARC coating on front surface of cell can reduces the reflection by enhancing absorption of light, which enhances the efficiency and Jsc value. The main Optical losses from the front surface are the most significant impediment to better solar cell efficiency. In addition, there is a higher probability for visual loss during the photoelectric effect in solar cells, reducing the PCE of solar cells [29]. It is observed that the influence of the ARC layer in the range of 500–700 nm wavelength is more suitable for spectral loss [30,31]. As a result, several ARC materials have been used to improve efficiency [32,33]. Layers are organized in descending order of band gap, highest band gap material is on top surface and bottom layer material should have low band gap as compared to other materials [34,35]. Energy of lower wavelength can be absorbed by a material which have larger band gap [10,36]. Refractive index is a significant parameter for ARC layer. The reflection of radiation from the surface will effectively decreases if refractive index of antireflection coating (ARC) is the geometrical mean of two surrounding indices. Refractive index of ZnO at 600 nm wavelength is 2 [7] and 1 for air. The ZnO refractive index is near ideal, which is needed for the ARC layer for the Si-based solar cell. So, ZnO coating can also be replaced with ARC for silicon wafers if the film thickness is optimized for peak spectrum wavelength. The peak intensity of solar radiation is about 600 nm. The Fresnel equation for normal incidence showed that ZnO had a refractive index of 2 at 600 nm. Since extinction coefficient of ZnO at 600 nm was examined and found to be modest, it was not considered while doing the calculations. Air was supposed to have a refractive index of 1. At 600 nm wavelength, silicon has a refractive index of 3.95. If the refractive index of the anti-reflection layer is the geometrical mean of neighboring materials, then the reflection is minimum. Considering silicon is on one side and air on another, the refractive index of ARC at 600 nm wavelength is 1.99 in the solar spectrum. In our case, we are considering the different ARC materials on the ZnO window layer to minimize reflection and enhance efficiency. In this case, if we consider ZnO on one side and air on another side using **eq- 2** ideal value is 1.41. The refractive index of magnesium fluoride (MgF_2) is 1.38, which is near to ideal refractive index for ZnO/Si. The required thickness of the ARC layer can be calculated by **eq-1**. Applying quarter-wavelength ARC, commonly employed on the front surface, is one popular way [37]. The thickness of the ARClayer was calculated by the refractive index and the wavelength of the ARC material [38]. For a quarter-wavelength anti-reflection coating, light fall on the ARC layer with freespace wavelength (λ_0) and refractive index (η_1) for transparent material are considered, thickness (d) is estimated by eq. (1) and (2) [39].

$$d = \frac{\lambda_0}{4\eta_1} \tag{1}$$

And [39].

$$\eta_1 = \sqrt{\eta_0 \eta_2} \tag{2}$$

where, η_0 an $d\eta_2$ is the refractive index of the air and window layer [39].

The influence of changing window and absorber layer thickness and doping concentration with a single ARC layer on the performance of ZnO/Si solar cells was studied in this manuscript. The materials such as magnesium oxide (MgO), aluminum trioxide (Al_2O_3), magnesium fluoride (MgF_2) and titanium nitride (TiN), with 1.72, 1.76, 1.38 and 1.78 refractive indexes [40–42] were used as ARC layer on the front surface of ZnO/Si solar cell. Using the thickness and refractive index of ARC materials, the optical and photovoltaic characteristics have been extracted by software named PC1D.The PC1D is a simulation tool for solar cells with a simple interface defining the problem. The influence of the thickness of layers, diffusion length, photogeneration, doping concentration and minority carrier life time on the operation of ZnO/Si-based solar cells have been premeditated by PC1D.The PC1Dwas established by a group of scientist working in UNSW (University of south

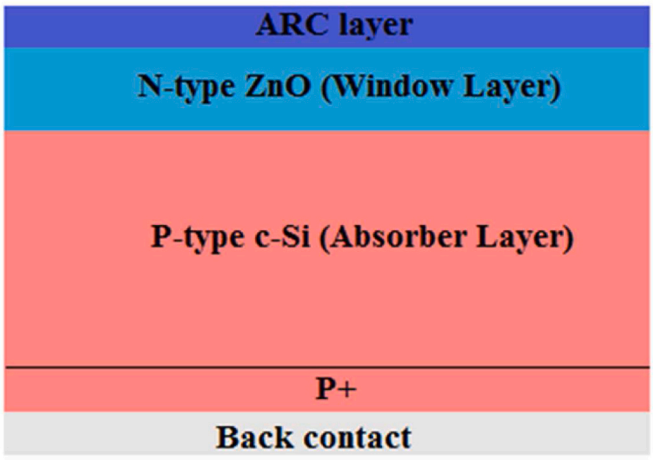

Fig. 1. Schematic diagram of the proposed model.

Table 1
Parameter of optimum stimulated case.

Parameters	Values
Front Region (Window layer ZnO)	
Emitter Thickness	0.5–6 μm
Band gap	3.27 eV [8]
Refractive index	2
Electron affinity	4.35 [49]
Dielectric Constant	8.66
Doping concentration (N-Type)	2.2×10^{19}cm^{-3}
Electron mobility	50 cm^2/Vs
Bulk recombination	$\tau_n = \tau_p = 1 \times 10^{-6}$ μs [7]
Front-surface recombination	S_n=S_P =1×10^7 cm s^{-1} [7]
Rear Region (Absorber layer Si)	
Base thickness	60–200 μm
Band gap	1.124 eV [1]
Dielectric constant	11.9
Doping concentration (P-Type)	5×10^{16}cm^{-3}
Peak 1st rear diffusion (P-Type)	3×10^{18}cm^{-3}
Bulk recombination	100μs
Front surface recombination	S_n=S_P =1×10^6 cm s^{-1}
Rear surface recombination	S_n=S_P =300 cm s^{-1}
Other parameters	Internal PC1D

wales) [34,35,43]. This tool allows to simulate of the different parameters of semiconductor devices, and it includes library files of electron affinity, dielectric constant, carrier lifetimes, electron-hole motilities, doping concentration, refractive index, and bandgap for InP, GIN, Ge, GaAs, AlGaAs, a-Si and a-Si based devices [44,45].

2. Proposed model using ZnO and device simulation parameters

ZnO is a direct wide band gap materials with a bandgap that can be modified by alloying or doping from 3 to 5 eV. The critical characteristics of ZnO that distinguish it from other II–VI and III–V wide band gap materials include its low processing cost low toxicity, and very stable wurtzite structure with a lattice c/a ratio of 1.603, very close to the ideal ratio of 1.633 [46]. ZnO's more considerable exciton binding energy (60 meV) ensures effective photovoltaic and luminescent characteristics [47]. Additionally, ZnO is more radiation-resistant than GaAs, GaN, and Si, which prevents sunlight-induced degradation and ensures a longer lifespan. Gallium or aluminum doped ZnO has lately attracted attention as a feasible replacement for indium tin oxide in transparent conducting oxides (TCOs).

Our proposed model for absorber layer P-type silicon wafer and window layer n-type ZnO was chosen, and ZnO is sandwiched between the p-Si and ARC layer as demonstrated in Fig. 1. The arrangement of solar cell layers follows a hierarchy of band gap energy materials, whereby the top surface exhibits the highest band gap energy and the bottom surface displays the lowest band gap energy [34,35]. This is because a material with a large bandgap has the ability to absorb the lower wavelengths of solar radiation [10,36]. As a result, the ZnO layer's transparency in the visible and infrared regions is significant. Nayaketal [48]. reported the gallium-doped ZnO thin film using the well-known technique (sol-gel spin coating) for device applications. The transparency of thin films with 3.3×10^{-3} Ω cm resistivity was more than 80% in the visible region with 2 at% of Ga.

For solar cell fabrication, PC1D has several adjustable parameters that can be iterated to achieve an optimized window. In PC1D software, internal parameters like refractive index, electron affinity, band gap, electron-hole mobility, dielectric constant, carrier lifetimes and doping concentration, etc., are used to simulate various types of the solar cell. All device parameters are given in Table 1. The simulation is carried under 1.5 air mass and constant sun intensity (0.1 W/cm^2). The carrier's excitation at 25 °C ambient temperature is parted into 16-time steps. The thicknesses of the proposed device's window layer and absorber layer range from 0.5 to 6 μm and 60–200 μm, respectively and parameters of ZnO/Si solar cell are selected from previously reported articles.

3. Photovoltaic properties

The basic four parameters evaluate overall performance fill factor (FF), short circuit (I_{sc}), open circuit voltage (V_{oc}) and PCE (%) of the solar cell. Short-circuit current density (J_{sc}) is stated usually (J_{sc} = I_{sc}/area) in consideration of the dependence on the junction area. V_{oc} stands for the greatest voltage that a solar cell can produce with no current flowing. The term "FF" refers to the relationship between the greatest power density that may be extracted from a solar cell and the product of V_{oc} and J_{sc}. The most straightforward measurement is PCE **eq-3**, or the ratio of output energy to input energy[50].

$$\mathrm{PCE} = \frac{P_m}{P_{in}} \times 100\% = V_{oc} \times J_{sc} \times FF \times 100\% \tag{3}$$

Where, P_{in} is the input energy from the sun (0.1 W/cm^2) for standard-test irradiation AM1.5 G), P_m is the output energy. Quantum efficiency is also significant in estimating the I_{sc} and performance in a specific wavelength range. The modelling competencies of PC1D simulation were utilized to study the PV characteristics such as current, power-voltage and quantum efficiency by analyzing the optical characteristics of ZnO/Si heterojunction solar cells.

The following equation determines the values of photocurrent produced by solar cells [50].

$$I_L = Q \int_0^{\infty} QE(E)N(E)(1 - R(E))dE \tag{4}$$

where, R(E) = reflectance, QE (E) = internal quantum efficiency, and N (E) = incident photon flux density. Generally, semiconductor materials cannot absorb low energy photons[50].

4. Result and discussion

4.1. Optimization of absorber and window layer thickness

The absorber and window layer thickness are key parameters to attain maximum efficiency [51]. It has been discovered that even minor variations in thickness of absorber layer cause considerable variations in V_{oc} and I_{sc}, which influence the c-Si based solar cells performance [52]. The absorber layer of the SHJ is known to be a weakly doped region when associated to the other regions of solar cells. In general, the formation of heterojunctions between the c-Si and oxide often overwhelms the obstacles at front and rear interfaces for higher carrier transport [53]. By thinning of the top layer, the large amount of radiation is absorbed, and large fraction of carriers within diffusion length is

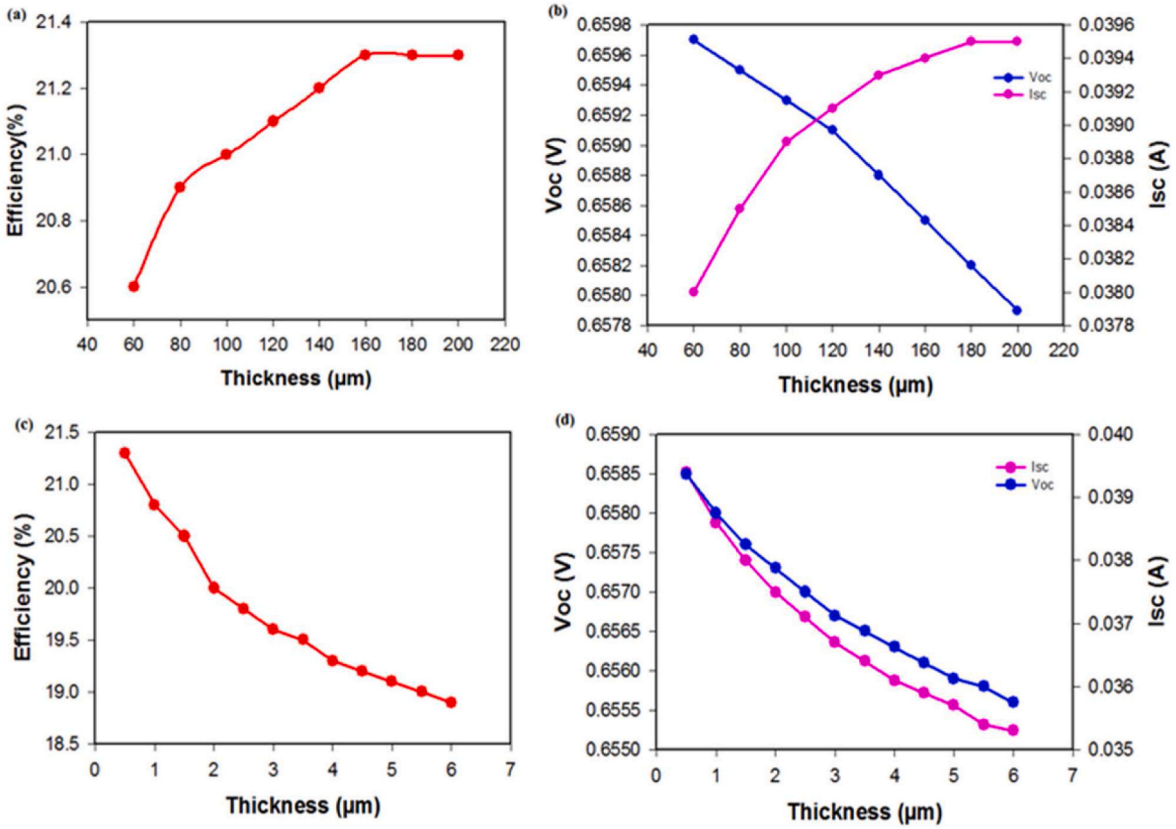

Fig. 2. Optimization of the thickness in term of (a) efficiency for absorber layer (b) Voc and Isc for absorber layer (c) efficiency for window layer (d) Voc and Isc for window layer.

generated by the incident sunlight [54]. PC1D software is used to optimize the thickness of base and window region by using simulation parameters. The influence of ZnO and Si thickness on I_{sc} and V_{oc} and conversion efficiency (η) are depicted in Fig. 2. The recombination process speeds up with the increment in absorber layer thickness so affect the overall PV devices performance. According to the nature of solar cell, I_{sc} increases and V_{oc} decreases with an increase of absorber layer thickness. The highest value of V_{oc} and I_{sc} was recorded to be 0.6597 V for 60 μm thickness and 0.0395 A for 200 μm thickness as illustrated in Fig. 2 (b). It is visible from Fig. 2(d) that short circuit current (I_{sc}) reduces monotonically as the thickness of ZnO increases due to significant drop in number of available photons in the space charge region. The silicon material exhibits a significant space charge region owing to the substantial doping variability between the two materials. It is observed that the carrier production is predominantly contributed by photons reaching silicon. Absorption in a thicker window layer reduces I_{sc} because I_{sc} is directly related to photogenerated carriers. The same mechanism can be used to explain a drop in V_{oc} as ZnO thickness increases. The highest observed values of V_{oc} and I_{sc} are 0.6585 A and 0.0394 V at 0.5 nm thickness of ZnO layer as illustrated in Fig. 2(d).

The increment in the absorber layer thickness can absorb more sun light and hence increase the charge carriers [55]. The increase in device parameter values is due to enhanced photon absorption and hole-electron production in the absorber layer. Insufficient thickness of the absorber layer leads to reduced efficiency due to inadequate absorption of the maximum incoming solar radiation. Nevertheless, in cases where the thickness of the absorber layer surpasses the optimal value, the path length traversed by the photo-generated carriers increases, leading to a greater degree of recombination [56]. It has been observed that increasing the thickness of absorber layer enhances the PCE (%). Initially, as the thickness of the absorber layer is increased up to 160 μm, the efficiency increases until it approaches to a stable value. The maximum efficiency of 21.3% has been achieved with thickness of 160 μm as shown in Fig. 2 (a). For thicker absorber layer (values greater than 160 μm) does not necessarily improve overall cell performance so the thickness of 160 μm is chosen as an optimum thickness for efficient and low cost HJ solar cell. The recombination loss influences the performance of cell [55] that can be altered by varying window layer thickness from 0.5 μm to 6 μm. Moreover, the result indicates that η (%) was decreased as the window layer thickness increased. The maximum efficiency of 21.3% was achieved with 0.5 μm thickness of window layer and decreased to 18.9% by further increase to 6 μm as demonstrated in Fig. 2(c). The higher window layer thickness could distort interface to metal layer, by making barriers for appropriate charge collection [57].

4.1.1. Optimization of doping carrier concentration of window or absorber layer

The doping carrier concentrations in window or absorber layer play a vital role in attaining high Voc and Isc of solar cell [39]. High doping concentration can usually destroy structure layer due to generation of undesired shunt path on absorber layer of solar cell [58]. The doping concentration should be optimized without any negative influence for high performance. The doping carrier concentration varies in range of 10^{14} to 10^{18} cm^{-3} for absorber layer and 10^{17} to 10^{21} cm^{-3} for window layer. The Efficiency, Voc and Isc against the doping carrier concentration of window and absorber layers illustrated in Fig. 3. The drop in efficiency and Voc with the increment in doping concentration from 10^{16} cm^{-3} in absorber layer may be related with variation in band energy levels and band gap structures. The constant value of Isc = 0.0397 A has been observed in the range of 10^{14} to 10^{15} cm^{-3} and it starts decreasing on further increase in doping concentration. For window layer value of Isc is independent of doping concentration for 10^{17} to $10^{21}cm^{-3}$. A constant value of 0.0394 A has been recorded for window layer. The value of efficiency and Voc increases as the doping

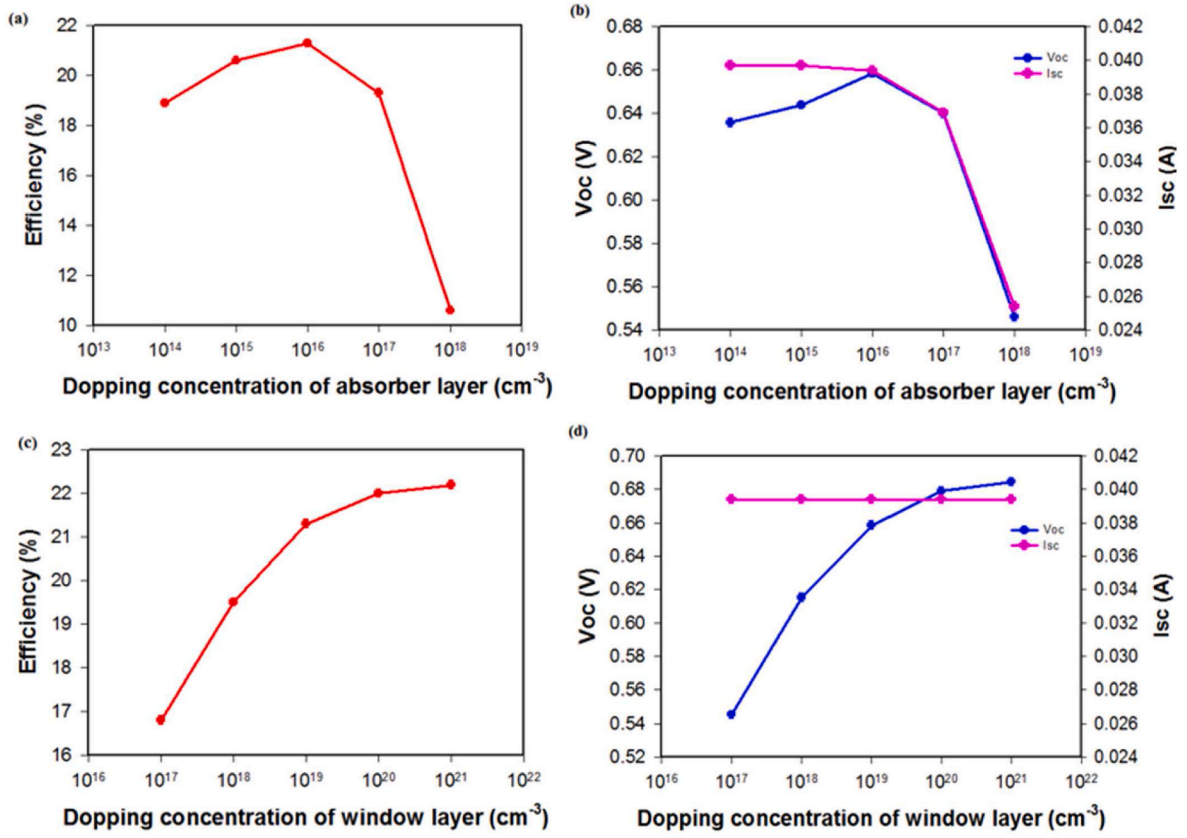

Fig. 3. Optimization of the doping concentration in term of (a) efficiency for absorber layer (b) Voc and Isc for absorber layer (c) efficiency for window layer (d) Voc and Isc for window layer.

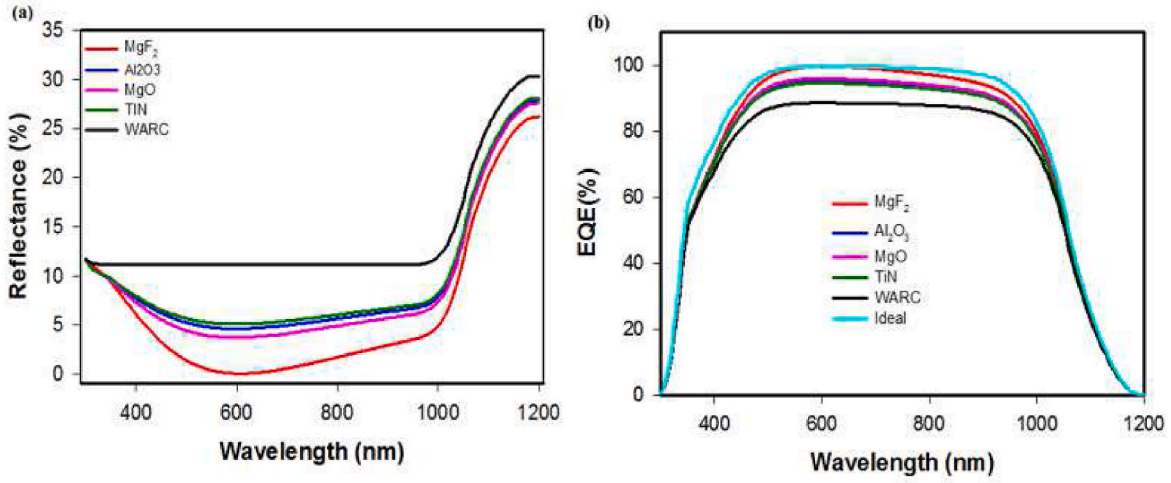

Fig. 4. (a) Reflectance analysis and (b) External quantum efficiency of different SLARC materials.

concentration of window layer increases. It is important to point out that crystallographic defects increases as the value of doping carrier concentration increases and it decreases the carrier lifetime. So, the diffusion coefficient decreases. The pronounced effect of high doping concentration is band gap narrowing. So optimized doping concentration should be taken for window and absorber layer. Maximum efficiency of 21.3% with 5×10^{16} cm^{-3} doping concentration for absorber layer is recorded it shows a good agreement with previous published article [1]. For window layer 2.2×10^{19} cm^{-3} doping concentration has been chosen to improve the PCE (%) of solar cell without negative impact the results shows a good agreement with pervious article [7].

4.2. *Influence of ARC layers on n-ZnO/Si solar cell*

Anti-reflection coating layer improves overall performance by increasing short circuit current and reducing the reflectance attained by absorbing the photons from incoming light of solar cell [41,59]. The reflectance is an important optical property that influences the efficiency and the average reflectance (Rav) of different materials like MgF_2, Al_2O_3, MgO and TiN, are 1.91%, 5.69%, 4.95% and 6.09% in

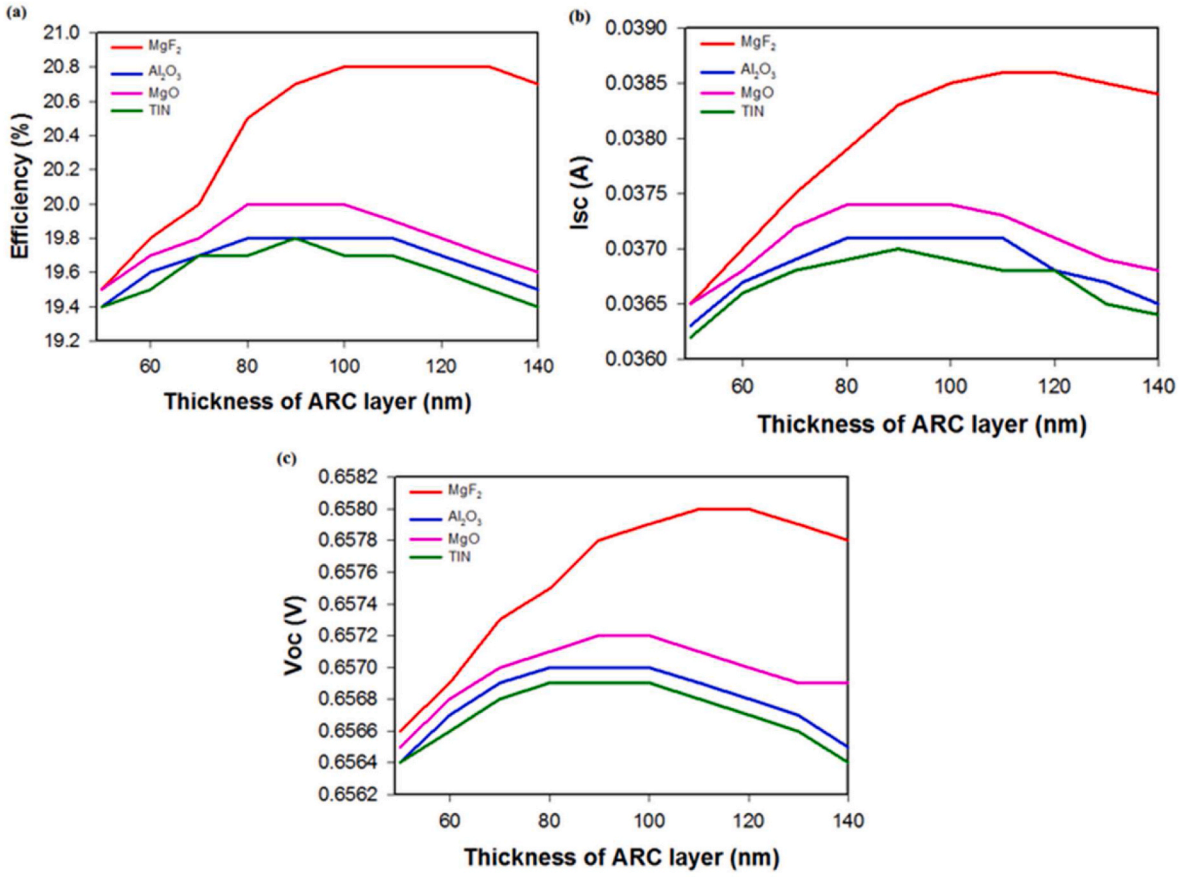

Fig. 5. Optimization of different anti-reflection coatings layer thickness in term of (a) Efficiency (b) I_{sc} (c) V_{oc}.

400–1000 nm. The Rav is 11.13% without any ARC layer in the same wavelength range but a significant drop in Rav to 1.91% and as lowest reflectance of 0.064% at 600 nm has been recorded after applying MgF_2 as SLARC as shown in Fig. 4. Reflectance curve of without any anti-reflection layer is shows by black curve. The red curve shows the reflectance curve for MgF_2 ARC materials that are near to ideal case (zero % reflectance). The curve exhibits a sharp decline until a particular threshold, followed by a subsequent rise.

The quantum efficiency of a solar cell refers to the proportion of charge carriers that are absorbed by the cell in relation to the number of photons with a specific energy level that impinge upon it [60]. The external quantum efficiency is about 87% without any ARC material, and it has been improved significantly upto 98% by applying MgF_2 layer in the range of 450–1000 nm (Fig. 4(b)). The absorption of blue photons often occurs in the uppermost region of the anti-reflection coating where all carriers are anticipated to travel through whole layer in order to approach p-n junction. From Fig. 4 (b), it is clear that the use of ARC layer enhances the EQE. This influence might be attributed to reduction in reflection by application of ARC layer and the EQE of n-ZnO/p-Si solar cell has reached to its maximum value for MgF_2 ARC layer. Surface passivation improves the overall external quantum efficiency by lowering the number of dangling bonds, which reduces recombination

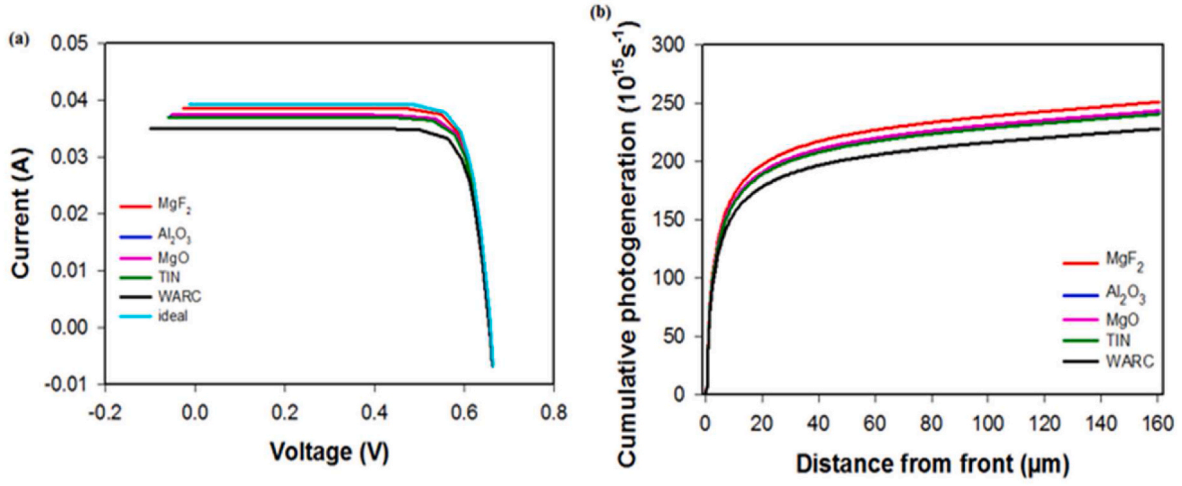

Fig. .6. (a) Analysis of I–V (b) Cumulative photogeneration rate for solar cells with different ARC materials.

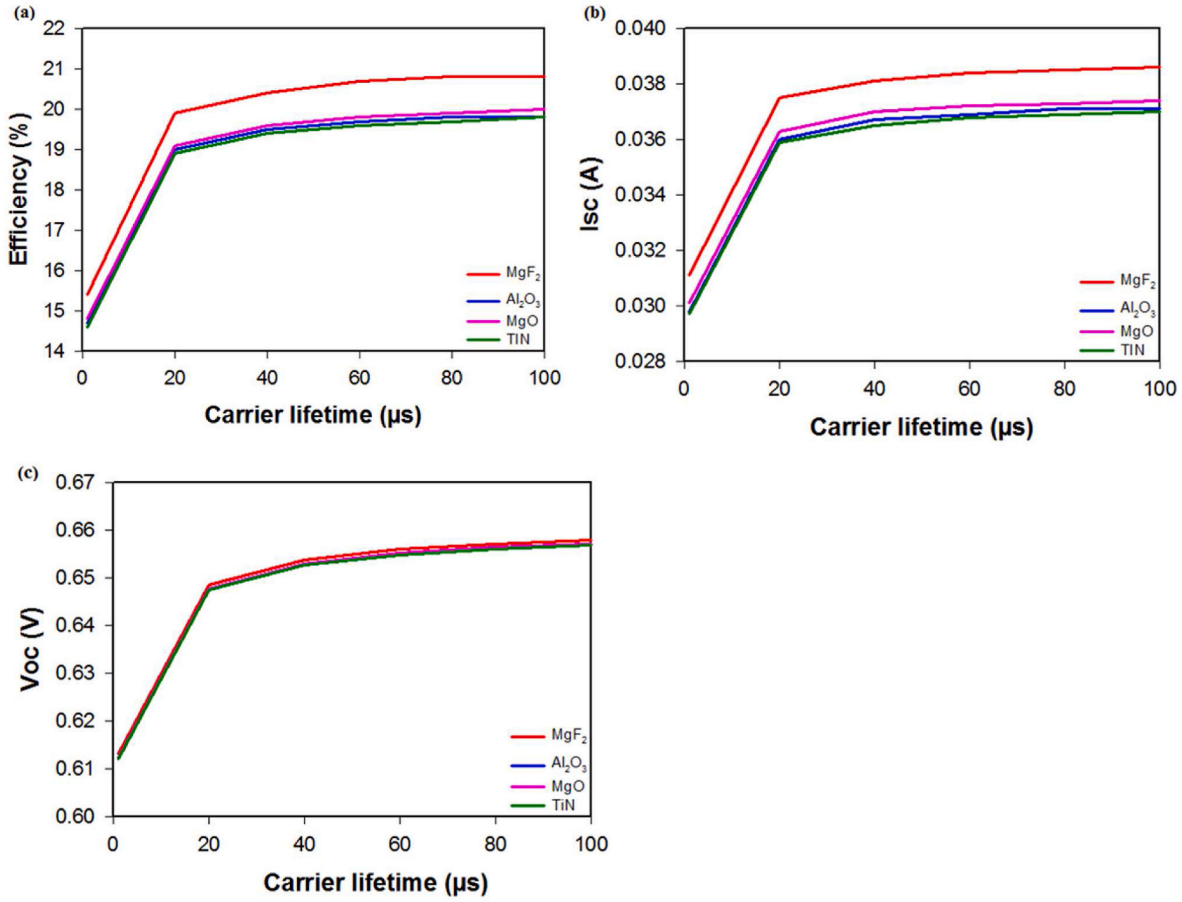

Fig. 7. Optimization of carrier lifetime for different ARC layer in terms of (a) Efficiency (b) Isc (c) Voc.

effects [61].

The thickness of various ARC layers across the simulation has been varied between 50 nm −140 nm. The efficiency improves as the thickness of ARC layers increases until optimized ARC thickness after that on further increase in ARC layer thickness it again starts decreasing. It is reasonable to suppose that the optimal thickness of ARC layer might be related to the generation of suitable refractive index and a significant reduction in reflection which leads to charge extraction on front surface and maximum absorption. We have analyzed the impact of thickness of different ARC materials on Voc and Isc as shown on Fig. 5. Among all ARC materials the maximum value of V_{OC} of 0.6580 V, $I_{SC}$of 0.0386 A, and efficiency of 20.8% for MgF_2 ARC layer have been recorded at optimized thickness of 110 nm. Similarly, efficiencies recorded for Al_2O_3, MgO and TiN, are 19.8%, 20.0% and 19.8%, respectively. To obtain the maximum efficiency for Al_2O_3, MgO and TiN 85 nm, 87 nm and 84 nm is the optimal thickness.

The current voltage characteristics are ultimate criterion for confirming the effective use of ARC layer in ZnO/Si-based solar cells. The ZnO/Si based solar cell without any anti-reflection coatings layer shows V_{oc} value that is 0.6555 and the value of I_{sc} is 0.0350 A and efficiency is 18.8% while a significant increment in photovoltaic characteristics such as value of Voc is 0.6580 V, the value of Isc is 0.0386 A and efficiency of 20.8% is recorded in ZnO/Si based solar cell with MgF_2 ARC material as shown in Fig. 6(a). The MgF_2 ARC layer (110 nm thickness) shows highest efficiency with V_{oc} and I_{sc} value as observed in Fig. 6. Improvement in photovoltaic parameters with ARC layer of MgF_2 is attributed to significant drop in reflectance from 11.13% to 1.91% after ARC layer of MgF_2.

The recombination and cumulative photogeneration rates are essential parameters to estimate the charge collection and high charge extraction of solar cell [62]. The cumulative photogeneration rates are estimated by number of the electrons produced in each region mainly due to photons absorption [63]. The photogeneration rate was investigated with and without ARC layer. Fig. 5 (b) represents the relation between emitter depth and cumulative photogeneration rates with ARC layers for solar cell. The photogeneration rate initiates from zero and gradually enhances with the thickness of front distance. The photogeneration rate ($2.51 \times 10^{17} s^{-1}$) with MgF_2 was greater than other layers; however, without any ARC layer low photogeneration rate of $2.28 \times 10^{17} s^{-1}$ was observed for ideal case it was $2.57 \times 10^{17} s^{-1}$.

Carrier lifetime plays a vital role to attain the high η (%) of solar cells. In general, the carrier lifetime of photon absorber surface in a silicon based solar cell has a significant impact on PV characteristics [58]. The huge agglomeration of charges on electrodes instantly enhances the efficiency. Recombination and lifetime is crucial for the collection of high number of charge carriers [3,64]. Moreover, it is essential to minimize the carrier recombination which enhances the carrier lifetime [34,65]. A semiconductor device's charge carrier lifetime depends on recombination rate, which is regulated by concentration of minority charge carriers. The semiconductor materials with passivation and indirect band gap properties control the recombination process [1,66–69]. The value I_{sc} and η (%) of solar cell increases with carrier lifetime [63]. The value η (%) increased in all ARC layers when carrier lifetime was increased (1 μs- 100 μs). When carrier lifetime is longer, the probability of carrier to reach its destination before recombination increases [70]. The carrier lifetime of different ARC layer against efficiency, V_{oc} and I_{sc} values are shown in Fig. 7. The optimum carrier lifetime is essential because carrier lifetime is essential parameter for maximum solar cell performance. From results, it is confirmed that efficiency, I_{sc} and V_{oc} increases as the carrier lifetime increases upto 1–100 μs. Among all ARC

Table 2
Optoelectrical properties of ZnO/Si solar cell with different ARC Materials.

ARC Material	R_{av} (%)	Refractive index	Thickness (nm)	Voc (V)	Isc (A)	FF (%)	η (%)
MgF_2	1.91	1.38	110	0.6580	0.0386	82	20.8
Al_2O_3	5.69	1.76	85	0.6570	0.0371	81	19.8
MgO	4.95	1.72	87	0.6572	0.0374	81	20.0
TiN	6.09	1.78	84	0.6569	0.0370	81	19.8
WARC	11.13	–	–	0.6555	0.0350	82	18.8
Zno/Si	–	–	–	0.6585	0.0394	82	21.3

Table 3
Comparative analysis of reported ZnO/Si based solar cell.

Solar cell types	Isc (A)	V_{oc} (V)	FF (%)	Efficiency (%)	Reference
ZnO/Si	0.02826	0.360	86.19	5.91	[71]
ZnO/Si	0.038	0.520	71.00	14.0	[17]
Al–ZnO/MIG-Si	0.01854	0.670	85.15	10.35	[71]
ZnO/Si	0.0377	0.6221	81	19	[7]
Mg ZnO/Si	0.03303	0.312	58	5.93	[23]
Si/ZnO	0.03157	0.465	78.76	11.57	[20]
Si/Mg ZnO	0.03139	0.566	81.46	14.46	[20]
Without ARC	0.035	0.6555	82	18.8	This work
With MgF_2 ARC	0.0386	0.6580	82	20.8	This work
ZnO/Si	0.0394	0.6585	82	21.3	This work

layer MgF_2 showed maximum efficiency with maximum values of V_{oc} = 0.6580 V and I_{sc} = 0.0386 A at 100 μs carrier lifetime. Moreover, linear increase in the efficiency, I_{sc} and V_{oc} with carrier lifetime of maximum 100 μs is observed and hence optimum value of carrier lifetime is 100 μs. It is observed that MgF_2 with thickness of 110 nm poses maximum efficiency with corresponding values of V_{oc} and I_{sc}. The optimum numerical values for purposed MgF_2/ZnO/Si solar cells have been given in Tables 2 and 3. The enhancement in photovoltaic characteristics for ZnO/Si with MgF_2 ARC layer has been attributed to considerable deduction of reflection from 11.13% to 1.91% with MgF_2 ARC layer. This study establishes the impact of ARC layer thickness, window and absorber layer and carrier lifetime on PV characteristics of proposed ZnO/Si solar cell. In addition, the comparative analysis of optoelectronic properties has been presented in Table 3 of ZnO/Si solar cells.

5. Conclusion

The computational study of the doping concentration of window and absorber layer, carrier lifetime, thickness of ARC, window and absorber layer has been successfully carried out for ZnO/Si solar cell. It is revealed from results that PCE of 21.3% achieved at optimum thickness and doping concentration of window and absorber layer at zero reflectance. In this study the influence of different ARC layers as single layer upon the performance of solar cell was also analyzed by simulation (PC1D). The results of this study have confirmed that MgF_2 as single ARC layer with optimum thickness of 110 nm and carrier lifetime of 100 μs and maximum PCE of 20.8% in comparison of Al_2O_3, MgO and TIN. Without any ARC layer it showed that 18.8% with Voc of 0.6555 V and Isc of 0.0350 A. The results of this computational study evidenced that the manufacturing of low cost ZnO/Si solar cell with maximum conversion efficiency can be achieved by cost effective AR materials. The application of different AR materials in ZnO/Si solar cells can provides a meaningful contribution in this field.

Declaration of competing interest

The authors declare that they have no known competing financial interests or personal relationships that could have appeared to influence the work reported in this paper.

References

[1] X. Cai, et al., An in-depth analysis of the silicon solar cell key parameters' optimal magnitudes using PC1D simulations, Optik 164 (2018) 105–113.
[2] T. Koida, High-mobility transparent conductive oxide layers, in: Spectroscopic Ellipsometry for Photovoltaics, Springer, 2018, pp. 565–586.
[3] H. Naim, et al., An in-depth optimization of thickness of base and emitter of ZnO/Si heterojunction-based crystalline silicon solar cell: a simulation method, J. Electron. Mater. 51 (2) (2022) 586–593.
[4] S. Roguai, A. Djelloul, A structural and optical properties of Cu-doped ZnO films prepared by spray pyrolysis, Appl. Phys. A 126 (2) (2020) 1–8.
[5] D.K. Shah, et al., Effect of Ag doping in double antireflection layer on crystalline silicon solar cells, Nanosci. Nanotechnol. Lett. 11 (2) (2019) 159–167.
[6] V.A. Coleman, C. Jagadish, Basic properties and applications of ZnO, in: Zinc Oxide Bulk, Thin Films and Nanostructures, Elsevier, 2006, pp. 1–20.
[7] B. Hussain, A. Ebong, I. Ferguson, Zinc oxide as an active n-layer and antireflection coating for silicon based heterojunction solar cell, Sol. Energy Mater. Sol. Cell. 139 (2015) 95–100.
[8] B. Hussain, A. Ebong, I. Ferguson, Zinc oxide and silicon based heterojunction solar cell model, in: 2015 IEEE 42nd Photovoltaic Specialist Conference (PVSC), IEEE, 2015.
[9] L.G. Gerling, et al., Characterization of transition metal oxide/silicon heterojunctions for solar cell applications, Appl. Sci. 5 (4) (2015) 695–705.
[10] M. Labed, et al., Study on the improvement of the open-circuit voltage of NiOx/Si heterojunction solar cell, Opt. Mater. 120 (2021), 111453.
[11] S. Tohoda, et al., Future directions for higher-efficiency HIT solar cells using a Thin Silicon Wafer, J. Non-Cryst. Solids 358 (17) (2012) 2219–2222.
[12] H. Sayed, et al., Theoretical analysis of optical properties for amorphous silicon solar cells with adding anti-reflective coating photonic crystals, in: Photonics, MDPI, 2022.
[13] L. Korte, et al., Solar energy material &amp, Sol. Cell. 93 (2009) 905.
[14] S.-Y. Lien, et al., Influence of surface morphology on the effective lifetime and performance of silicon heterojunction solar cell, Int. J. Photoenergy 2015 (2015).
[15] L. Chen, et al., Research on ZnO/Si heterojunction solar cells, J. Semiconduct. 38 (5) (2017), 054005.
[16] N. Ziani, M. Belkaid, Computer Modeling Zinc oxide/silicon Heterojunction solar cells, 2018.
[17] R. Pietruszka, et al., ZnO/Si heterojunction solar cell fabricated by atomic layer deposition and hydrothermal methods, Sol. Energy 155 (2017) 1282–1288.
[18] D.K. Shah, et al., Influence of minority charge carrier lifetime and concentration on crystalline silicon solar cells based on double antireflection coating: a simulation study, Opt. Mater. 121 (2021), 111500.
[19] S.C. Das, et al., Band gap tuning in ZnO through Ni doping via spray pyrolysis, J. Phys. Chem. C 117 (24) (2013) 12745–12753.
[20] S. Vallisree, R. Thangavel, l.T. Lenka, Modelling, simulation, optimization of Si/ZnO and Si/ZnMgO heterojunction solar cells, Mater. Res. Express 6 (2) (2018), 025910.
[21] S. Tyagi, P.K. Singh, A.K. Tiwari, Photovoltaic parameter extraction and optimisation of ZnO/GO based hybrid solar trigeneration system using SCAPS 1D, Energy Sustain. Dev. 70 (2022) 205–224.
[22] S. Boudour, et al., Optimization of defected ZnO/Si/Cu2O heterostructure solar cell, Opt. Mater. 98 (2019), 109433.
[23] S.S.A. Askari, M. Kumar, M.K. Das, Numerical study on the interface properties of a ZnO/c-Si heterojunction solar cell, Semicond. Sci. Technol. 33 (11) (2018), 115003.
[24] J. Gulomov, et al., Investigation of n-ZnO/p-Si and n-TiO 2/p-Si Heterojunction solar cells: TCAD+ DFT, IEEE Access, 2023.
[25] L. Mandal, et al., Analysis of ZnO/Si heterojunction solar cell with interface defect, in: Advances in Computer, Communication and Control: Proceedings of ETES 2018, Springer, 2019.
[26] D. Das, L. Karmakar, Optimization of Si doping in ZnO thin films and fabrication of n-ZnO: Si/p-Si heterojunction solar cells, J. Alloys Compd. 824 (2020), 153902.
[27] A. Tavkhelidze, et al., Fermi-level tuning of G-doped layers, Nanomaterials 11 (2) (2021) 505.
[28] D.D. Smith, et al., Toward the practical limits of silicon solar cells, IEEE J. Photovoltaics 4 (6) (2014) 1465–1469.
[29] L. Kosyachenko, Possibilities to decrease the absorber thickness reducing optical and recombination losses in CdS/CdTe solar cells, Mater. Renew. Sustain. Energy 2 (3) (2013) 1–20.
[30] N. Shanmugam, et al., Anti-reflective coating materials: a holistic review from PV perspective, Energies 13 (10) (2020) 2631.

[31] H. Abdullah, A. Lennie, I. Ahmad, Modelling and simulation single layer anti-reflective coating of ZnO and ZnS for silicon solar cells using silvaco software, J. Appl. Sci. 9 (6) (2009) 1180–1184.
[32] K.S. Gour, et al., Cd-free Zn (O, S) as alternative buffer layer for chalcogenide and kesterite based thin films solar cells: a review, J. Nanosci. Nanotechnol. 20 (6) (2020) 3622–3635.
[33] N. Das, D. Chandrasekar, M.M.K. Khan, Light reflection loss reduction by nano-structured gratings for highly efficient next-generation gaas solar cells, Energies 13 (16) (2020) 4198.
[34] D.K. Shah, et al., A simulation approach for investigating the performances of cadmium telluride solar cells using doping concentrations, carrier lifetimes, thickness of layers, and band gaps, Sol. Energy 216 (2021) 259–265.
[35] D. Kc, et al., Numerical investigation of graphene as a back surface field layer on the performance of cadmium telluride solar cell, Molecules 26 (11) (2021) 3275.
[36] K. Dasgupta, et al., Mathematical modelling of a novel hetero-junction dual SIS ZnO-Si-SnO solar cell, Silicon (2021) 1–10.
[37] B.M. Phillips, P. Jiang, Engineered biomimicry: Chapter 12, in: Biomimetic Antireflection Surfaces, Elsevier Inc. Chapters, 2013.
[38] S.L. Moffitt, et al., Multifunctional optical coatings and light management for photovoltaics, in: Advanced Micro-and Nanomaterials for Photovoltaics, Elsevier, 2019, pp. 153–173.
[39] G. Hashmi, et al., Investigation of the impact of different ARC layers using PC1D simulation: application to crystalline silicon solar cells, J. Theor. Appl. Phys. 12 (4) (2018) 327–334.
[40] R. Sharma, G. Amit, V. Ajit, Effect of single and Double Layer antireflection coating to Enhance photovoltaic Efficiency of silicon solar, 2017.
[41] D. Kc, et al., Impact of different antireflection layers on cadmium telluride (CdTe) solar cells: a PC1D simulation study, J. Electron. Mater. 50 (4) (2021) 2199–2205.
[42] E. Shkondin, et al., High aspect ratio titanium nitride trench structures as plasmonic biosensor, Opt. Mater. Express 7 (11) (2017) 4171–4182.
[43] G. Hashmi, et al., Study of the enhancement of the efficiency of the monocrystalline silicon solar cell by optimizing effective parameters using PC1D simulation, Silicon 10 (4) (2018) 1653–1660.
[44] M. Belarbi, A. Benyoucef, B. Benyoucef, Simulation of the solar cells with PC1D, application to cells based on silicon, Adv. Energy: Int. J. 1 (3) (2014).
[45] K. Devendra, et al., Modelling and simulation of AlGaAs/GaAs solar cell, Am. J. Eng. Res 9 (2020) 218–223.
[46] B. Hussain, et al., Applications and synthesis of zinc oxide: an emerging wide bandgap material, in: 2013 High Capacity Optical Networks and Emerging/Enabling Technologies, IEEE, 2013.
[47] B. Hussain, et al., Is ZnO as a universal semiconductor material an oxymoron? Oxide-based Mater. Dev. V 8987 (2014) 225–238.
[48] P.K. Nayak, et al., Spin-coated Ga-doped ZnO transparent conducting thin films for organic light-emitting diodes, J. Phys. Appl. Phys. 42 (3) (2008), 035102.
[49] N. Al-Khalli, M. Aboud, N. Debbar, Theoretical study and design of n-ZnO/p-Si heterojunction MSM photodiode for optimized performance, Opt Laser. Technol. 133 (2021), 106564.
[50] Y. Liu, et al., High-efficiency silicon heterojunction solar cells: materials, devices and applications, Mater. Sci. Eng. R Rep. 142 (2020), 100579.
[51] K.K. Maurya, V.N. Singh, Enhancing the performance of an Sb2Se3-based solar cell by dual buffer layer, Sustainability 13 (21) (2021), 12320.
[52] M. Wolf, E. Ralph, Effect of thickness on short-circuit current of silicon solar cells, IEEE Trans. Electron. Dev. 12 (8) (1965) 470–474.
[53] M. Mikolášek, Silicon heterojunction solar cells: the key role of heterointerfaces and their impact on the performance, in: Nanostructured Solar Cells, IntechOpen, 2017.
[54] C. Battaglia, A. Cuevas, S. De Wolf, High-efficiency crystalline silicon solar cells: status and perspectives, Energy Environ. Sci. 9 (5) (2016) 1552–1576.
[55] S. Asahi, et al., Two-step photon up-conversion solar cells, Nat. Commun. 8 (1) (2017) 1–9.
[56] Z. Ali, et al., Towards the enhanced efficiency of ultrathin Sb2Se3 based solar cell with cubic silicon carbide (3C–SiC) buffer layer, Opt. Mater. 128 (2022), 112358.
[57] D.K. Shah, et al., A computational study of carrier lifetime, doping concentration, and thickness of window layer for GaAs solar cell based on Al2O3 antireflection layer, Sol. Energy 234 (2022) 330–337.
[58] K. Devendra, D.K. Shah, A. Shrivastava, Computational study on the performance of zinc selenide as window layer for efficient GaAs solar cell, Mater. Today: Proc. 49 (2022) 2580–2583.
[59] T. Zhang, et al., Electron transport and electrical properties in poly (p-phenylene vinylene): methanofullerene bulk-heterojunction solar cells, J. Nanoelectron. Optoelectron. 14 (2) (2019) 227–231.
[60] T. Markvart, L. Castañer, Principles of solar cell operation, in: Practical Handbook of Photovoltaics, Elsevier, 2012, pp. 7–31.
[61] M. Ju, et al., The effect of small pyramid texturing on the enhanced passivation and efficiency of single c-Si solar cells, RSC Adv. 6 (55) (2016) 49831–49838.
[62] S. Shao, M.A. Loi, The role of the interfaces in perovskite solar cells, Adv. Mater. Interfac. 7 (1) (2020), 1901469.
[63] M. Basher, M.K. Hossain, M. Akand, Effect of surface texturization on minority carrier lifetime and photovoltaic performance of monocrystalline silicon solar cell, Optik 176 (2019) 93–101.
[64] Z. Li, et al., Minimized surface deficiency on wide-bandgap perovskite for efficient indoor photovoltaics, Nano Energy 78 (2020), 105377.
[65] A. Vossier, B. Hirsch, J.M. Gordon, Is Auger recombination the ultimate performance limiter in concentrator solar cells? Appl. Phys. Lett. 97 (19) (2010), 193509.
[66] M. Fathil, et al., The impact of minority carrier lifetime and carrier concentration on the efficiency of CIGS solar cell, in: 2014 IEEE International Conference on Semiconductor Electronics (ICSE2014), IEEE, 2014.
[67] K. Misiakos, D. Tsamakis, Accurate measurements of the silicon intrinsic carrier density from 78 to 340 K, J. Appl. Phys. 74 (5) (1993) 3293–3297.
[68] K. Graff, H. Fischer, Carrier lifetime in silicon and its impact on solar cell characteristics, Solar Energy Conv. (1979) 173–211.
[69] Z. Bandić, et al., Electron diffusion length and lifetime in p-type GaN, Appl. Phys. Lett. 73 (22) (1998) 3276–3278.
[70] E. Alarousu, et al., Ultralong radiative states in hybrid perovskite crystals: compositions for submillimeter diffusion lengths, J. Phys. Chem. Lett. 8 (18) (2017) 4386–4390.
[71] E. Kozarsky, et al., Thin film ZnO/Si heterojunction solar cells: design and implementation, in: 2012 38th IEEE Photovoltaic Specialists Conference, IEEE, 2012.